

Articles

Outward K⁺ Current Densities and Kv1.5 Expression Are Reduced in Chronic Human Atrial Fibrillation

David R. Van Wagoner, Amber L. Pond, Patrick M. McCarthy,
James S. Trimmer, Jeanne M. Nerbonne

Author Affiliations

Correspondence to Jeanne M. Nerbonne, PhD, Department of Molecular Biology and Pharmacology, Washington University School of Medicine, 660 S Euclid Ave, St Louis, MO 63110. E-mail jnerbonn@pharmdec.wustl.edu

Abstract

Abstract Chronic atrial fibrillation is associated with a shortening of the atrial action potential duration and atrial refractory period. To test the hypothesis that these changes are mediated by changes in the density of specific atrial K⁺ currents, we compared the density of K⁺ currents in left and right atrial myocytes and the density of delayed rectifier K⁺ channel α -subunit proteins (Kv1.5 and Kv2.1) in left and right atrial appendages from patients (n=28) in normal sinus rhythm with those from patients (n=15) in chronic atrial fibrillation (AF). Contrary to our expectations, nystatin-perforated patch recordings of whole-cell K⁺ currents revealed significant reductions in both the inactivating (I_{TO}) and sustained (I_{KSUS}) outward K⁺ current densities in left and right atrial myocytes isolated from patients in chronic AF, relative to the I_{TO} and I_{KSUS} densities in myocytes isolated from patients in normal sinus rhythm. Quantitative Western blot analysis revealed that although there was no change in the expression of the Kv2.1 protein, the expression of Kv1.5 protein was reduced by >50% in both the left and the right atrial appendages of AF patients. The finding that Kv1.5 expression is reduced in parallel with the reduction in delayed rectifier K⁺ current density is consistent with recent suggestions that Kv1.5 underlies the major component of the delayed rectifier K⁺ current in human atrial myocytes, the ultrarapid delayed rectifier K⁺ current, I_{Kur} . The unexpected finding of reduced voltage-gated outward K⁺ current densities in atrial myocytes from AF patients demonstrates the need to further examine the details of the electrophysiological remodeling that occurs during AF to enable more effective and safer therapeutic strategies to be developed.

Key Words:

K⁺ channels

atrial fibrillation

Kv1.5

Kv2.1

action potential duration

Atrial fibrillation is the most common chronic arrhythmia, present in 2% to 4% of the population over the age of 60. It is responsible for considerable patient discomfort, morbidity, and mortality.¹ Acute episodes of AF² and long-term

persistent AF³ are both marked by significant shortening in the effective refractory period of the atrium, shortening of the atrial action potential duration, and an increased dispersion of refractoriness. Although the clinically observed changes have been well documented and even reproduced in animal models,⁴ the underlying cellular changes in the atrium are still very poorly understood.

Atrial repolarization and refractoriness are parameters determined by the balance of inward Ca^{2+} and outward K^{+} currents. A decrease in action potential duration and effective refractory period during AF, therefore, would be expected to reflect (1) increased outward K^{+} current densities, (2) decreased inward Ca^{2+} current densities, or (3) increased outward K^{+} current density together with a decreased inward Ca^{2+} current density. As a beginning step to distinguish among these possibilities, the present study was undertaken to evaluate the impact of AF on the distribution and density of human atrial K^{+} currents. Several recent articles have now reported the normal distribution of human atrial K^{+} current components in a relatively comprehensive fashion, describing I_{TO} ,^{5 6} I_{Kur} ,⁷ I_{Kr} , and I_{Ks} .⁸ One of the primary K^{+} currents involved in atrial repolarization is I_{Kur} . This current has recently been suggested to correspond to the expression of the Kv1.5 α subunit,⁷ which has been cloned by several groups from human atrium.^{9 10} Therefore, we also examined Kv1.5 protein expression levels in membranes prepared from atrial appendages obtained from patients in NSR, as well as from patients who have been in AF until the time of surgery. The expression of another putative delayed rectifier K^{+} channel α subunit, Kv2.1, was also probed.

A combination of electrophysiological and biochemical techniques was used to quantify the density of atrial K^{+} currents and the expression of specific delayed rectifier K^{+} channel α subunits (Kv1.5 and Kv2.1). Contrary to our hypothesis, the electrophysiological experiments revealed that voltage-gated outward K^{+} current densities are significantly reduced in myocytes isolated from patients in chronic AF compared with the current densities in myocytes isolated from age-matched control patients in NSR. In addition, we show that the attenuation in K^{+} current density in myocytes from patients in AF is accompanied by a marked reduction in the expression of Kv1.5 but not Kv2.1 protein, consistent with the previous suggestions that Kv1.5 underlies the sustained component⁷ of the outward K^{+} current, I_{Kur} , in human atrial myocytes.

Materials and Methods

Patients

Atrial appendages were obtained as surgical specimens from patients undergoing cardiac bypass or cardiac transplantation surgery by following procedures approved by the Institutional Review Board. Left and right atrial appendages were obtained from 15 patients in chronic AF (>1 month at the time of surgery) undergoing mitral valve repair and/or the Maze procedure.¹¹ The AF population included 9 men and 6 women (mean age, 56 ± 3 years) (Table 1). Atrial appendages from two additional male patients (ages 40 and 61 years) who had experienced frequent episodes of PAF but were in NSR at the time of coronary bypass graft surgery were also included in the electrophysiological study.

View this table:

[In this window](#) [In a new window](#)

Table 1.

Clinical Characteristics of Patients Undergoing Surgery for Atrial Fibrillation

Control data were obtained from left and right atrial appendages obtained from 28 patients in NSR at the time of surgery (18 males, 10 females; mean age, 57 ± 2 years). This population included 17 patients undergoing routine cardiac bypass graft surgery, 6 transplant recipients (all with DCM), and 5 donors with nonfailing hearts with normal left ventricular function that were not used for transplantation because of the presence of underlying coronary artery disease or right ventricular contusions. All of the control patients were in NSR at the time of surgery. None of the bypass patients or nonfailing heart donors were on class III antiarrhythmic medications at the time of surgery; two of the transplant recipients were receiving amiodarone at the time of transplant. None of the control patients had a documented history of AF. The surgeries were performed between April 1995 and January 1997.

Atrial Myocyte Isolation Protocol

For both patient groups, atrial appendages were collected in either blood or saline and brought to the laboratory within 5 minutes of surgical excision. The tissue was rinsed in a dissection buffer containing (mmol/L) NaCl 140, KCl 5.4, MgCl₂ 1.2, HEPES 5, glucose 5, and BDM 30, pH 7.0. The tissue was cut into small chunks ($< 1 \text{ mm}^3$) with scissors. Tissue chunks were transferred to a 25-mL Erlenmeyer flask containing 10 mL of a Ca²⁺-free buffer with a composition similar to that of the dissection buffer, but lacking the BDM. The flask was placed in a water bath (30°C to 32°C) mounted over a magnetic stirrer. The minced tissue was washed three times for 4 minutes with the Ca²⁺-free buffer, followed by 10 mL of dissection buffer supplemented with 0.2% BSA, collagenase (Worthington type II [144 U/mg], 1 mg/mL), and protease (Sigma type XXIV, 0.4 mg/mL). After 45 minutes of exposure to enzymes, the supernatant was aspirated from the tissue and discarded. Fresh collagenase solution in dissection buffer (0.75 mg/mL, without protease) was added for an additional 10 minutes. The tissue was then triturated, and the chunks were allowed to settle. The digestion buffer was aspirated with a transfer pipette and centrifuged for 1 minute at 300 rpm ($\approx 18 \text{ g}$). The resulting supernatant was then discarded, and the myocyte pellet was resuspended in an incubation buffer containing (mmol/L) NaCl 118, KCl 4.8, MgCl₂ 1.2, CaCl₂ 0.5, KH₂PO₄ 1.2, glutamine 0.68, glucose 11, pyruvate 5, and BDM 10, along with 1 $\mu\text{mol/L}$ insulin, pH 7.2, and 1% BSA. The undigested tissue was placed in a fresh aliquot of collagenase solution for further digestion. This procedure was repeated three to five times, until the yield of viable myocytes began to decrease. After the final collection, the pooled myocytes were again centrifuged to remove residual collagenase/protease and resuspended in fresh incubation buffer. The myocytes were kept in a open plastic beaker under a 100% O₂ hood, at room temperature, until used, within 8 hours of isolation. Yields from this procedure were in the range of 10% to 30% for Ca²⁺-tolerant myocytes. Only well-striated, bleb-free, rod-shaped myocytes were used in the electrophysiological studies.

Perforated-Patch Whole-Cell Voltage- and Current-Clamp Recordings

The nystatin-perforated patch technique¹³ was used to avoid dialysis of cytosolic components and concomitant changes in ionic currents. Sylgard (Dow-Corning) coated low-resistance electrodes (2 to 4 M Ω , Corning 8161 glass; outer diameter,

1.65 mm; World Precision Instruments) were used as previously described.¹⁴ The composition of the pipette solution was (mmol/L) potassium methanesulfonate 100, KCl 40, K₂EGTA 5, MgCl₂ 2, and HEPES 10, pH 7.4. Nystatin was added to the pipette solution at a final concentration of 100 µg/mL, from a stock solution made fresh daily. Once nystatin was added to the buffer, the pipette solution was sonicated (30 seconds) and used within 3 hours.

Nystatin-free pipette solution was placed in the tip of the pipette by capillary action (3 to 4 seconds), and then nystatin-containing solution was backfilled in the pipette immediately before use. Junction potentials were nulled immediately before seal formation. After seal formation, increases in the capacitive response to a -10-mV step pulse (from a -50-mV holding potential) occur as nystatin perforates the patch. Cell capacitance and access resistance were checked throughout the experiment by tuning the patch-clamp amplifier with small square-wave voltage steps.

Only recordings from cells with low stable access resistance (<20 MΩ) and high seal resistance (>1GΩ) were included in the present study. Typical access resistance values were 9 to 12 MΩ. Electronic series resistance compensation (40% to 80%) was used to minimize voltage errors. With peak currents typically ≤1.6 nA, voltage errors resulting from the uncompensated series resistance were typically in the range 3 to 11 mV and were not corrected. No corrections were made for the negligible leak currents in these experiments. Data acquisition was performed with pClamp 6.0 software controlling either an Axopatch 200A or Axopatch 1C amplifier (Axon Instruments).

All experiments were performed on cells superfused with test solutions in a 35-mm culture dish mounted in a thermal stage controller (Biopatch ΔT system), maintained at a temperature of 30°C to 33°C, and gassed with 100% O₂. Solutions for whole-cell experiments were changed via a six-port gravity flow system. To keep the myocytes in position, the culture dishes were coated with laminin (Upstate Biotechnology, Inc; 6 µg per well) before use. The control bath solution contained (mmol/L) NaCl 135, KCl 5, sodium HEPES 5, sodium acetate 3, glucose 5, MgCl₂ 1, and CaCl₂ 1, pH 7.40. Nifedipine (2 µmol/L) was added to the bath solution to suppress voltage-gated Ca²⁺ currents. A holding potential of -50 mV was used to inactivate the voltage-dependent Na⁺ current.

Data analysis was performed using either the Clampfit module of pClamp or Origin (Microcal Software). Outward K⁺ conductances were measured as the slope of the current density-voltage relationship between the potentials of +10 to +70 mV. The current-voltage curves of both *I*_{TO} and *I*_{K_{SUS}} were very linear (*r*>.98) over this range of potentials. Current densities were determined by dividing current amplitudes by the whole-cell capacitance. *I*_{TO} was evaluated as the difference between the peak outward current density and the current at the end of a 450-millisecond voltage step (*I*_{K_{SUS}}). *I*_{K1} conductances were measured in the same manner, as the slope of the *I*_{K1} density-voltage plot in the voltage range of -70 to -90 mV.

Western Blotting of Human Atrial Membranes

Membrane proteins from human atrial appendages were isolated using a previously described method, developed, and used previously to obtain membrane proteins from rat atrial and ventricular tissue.¹⁵ Briefly, rapidly frozen (-80°C) samples of human atrial appendages, obtained as described above, were homogenized at 4°C in 10 vol of TE buffer containing 10 mmol/L Tris and 1 mmol/L EDTA, pH 7.4, using a Tekmar Tissuemizer homogenizer. All solutions contained the following protease inhibitors (mmol/L): iodoacetamide 1, phenanthroline 1, benzamidine 1,

and pefebloc 0.5, along with 4 $\mu\text{g}/\text{mL}$ aprotinin and 2 $\mu\text{g}/\text{mL}$ pepstatin. After homogenization, nuclei and debris were pelleted by centrifugation at 1000g for 10 minutes, and the supernatant was retained. The pellet was resuspended in TE, homogenized, and centrifuged again at 1000g for 10 minutes. The supernatants from both low-speed spins were pooled and centrifuged at 40 000g for 10 minutes. Pellets were resuspended in TE containing 0.6 mol/L KI and incubated on ice for 30 minutes. After centrifuging at 40 000g for an additional 10 minutes, the resulting pellets were twice more resuspended in TE and centrifuged at 40 000g. The resulting pellets were then solubilized in TE containing 2% Triton X-100 on ice for 1 hour. Insoluble material was centrifuged at 17 000g for 10 minutes. The protein content of each of the solubilized membrane preparations was determined using a BioRad DC protein assay kit. Solubilized membrane fractions were aliquoted and stored at -20°C until used.

Sample aliquots containing 25 μg protein were fractionated on 10% SDS-polyacrylamide gels and transferred to Hybond-PVDF membranes (Amersham Life Sciences). The membranes were immunoblotted using anti-Kv1.5 (1:100 final dilution)¹⁶ or anti-Kv2.1 (1:250 final dilution)¹⁷ antibodies. The membranes were washed in blocking buffer (PBS containing 0.2% I-block [Tropix] and 0.1% Tween-20) for 1 hour at room temperature and then incubated overnight at 4°C in primary antibody solution prepared in PBS containing 5% normal goat serum, 0.2% Triton X-100, and 0.1% NaN_3 . After incubation with the primary antibody, membranes were washed twice in blocking buffer for 10 minutes and subsequently incubated for 1 hour at room temperature in alkaline phosphatase-conjugated goat anti-rabbit IgG (Tropix) diluted 1:10 000 in blocking buffer. Membranes were then washed three times (15 minutes) in blocking buffer and twice (2 minutes) in assay buffer (Tropix, containing 0.1 mol/L diethanolamine and 1 mmol/L MgCl_2). Membrane-bound secondary antibodies were detected using the CSPD (Tropix) chemiluminescent alkaline phosphatase substrate and exposed to Scientific Imaging Film (Kodak). Films were scanned with a Molecular Dynamics personal densitometer and quantified with Image Quant software (Molecular Dynamics).

To facilitate comparison of samples for quantification purposes, an internal standard (10 ng rabbit IgG) was added to each membrane protein sample before the SDS-PAGE. Because the primary antibodies were raised in rabbits, the secondary antibody used for the Western blot analysis was alkaline phosphatase-conjugated goat anti-rabbit IgG; thus, this antibody detected both the primary antibody of interest and the rabbit IgG. The densities of the K^+ channel α -subunit bands and the rabbit IgG internal standard were corrected for background, and the ratio of the K^+ channel α subunit to the IgG was calculated for each sample.

Statistical Analyses

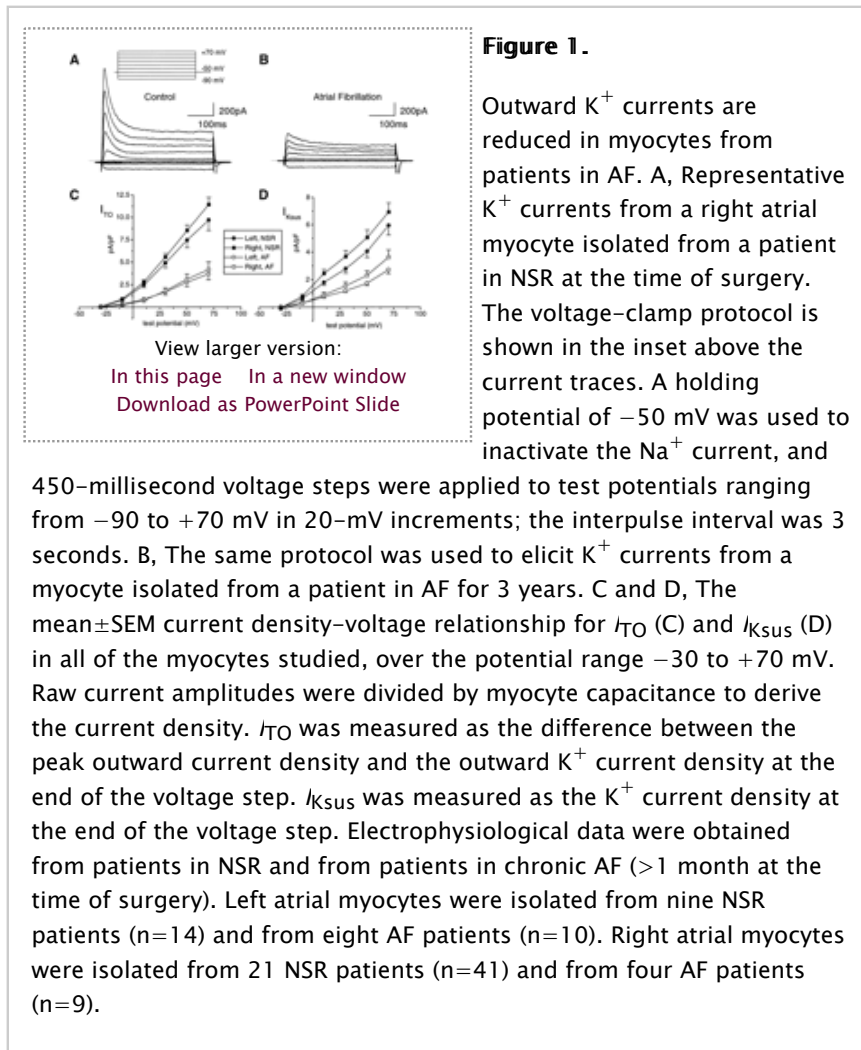
Differences between groups were evaluated using unpaired Student's *t* test. Statistical tests were deemed to be significant for values of $P < .05$. All results are presented as mean \pm SEM.

Results

Outward K^+ Currents Are Reduced in Chronic AF

In Fig 1A \downarrow , raw K^+ current records from a myocyte isolated from the right atrial appendage of a 56-year-old man in NSR are displayed. In Fig 1B \downarrow , similar current records from a myocyte isolated from a nondilated right atrial appendage from a 59-year-old woman in chronic AF for >3 years are presented. Although the myocytes were of similar size (104 pF in Fig 1A \downarrow , 115 pF in Fig 1B \downarrow), both the

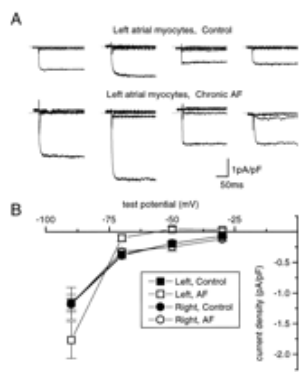
inactivating (I_{TO}) and sustained ($I_{K_{SUS}}$) outward K^+ current amplitudes were lower in the myocyte from the patient in AF. Interestingly, the amplitudes of I_{K1} , evoked during a step to -90 mV, were similar in both cells.



Similar electrophysiological recordings were obtained from myocytes isolated from both the left and right atria of patients who were either in NSR at the time of surgery ($n=28$ patients) or who had been in chronic AF for at least 1 month at the time of surgery ($n=11$ patients). Current amplitudes were measured in individual cells, and current densities were determined (as described in “Materials and Methods”) to normalize for differences in myocyte size. The mean \pm SEM current density versus voltage relations for I_{TO} are shown in Fig 1C \uparrow , and the mean \pm SEM current density versus voltage relations for the sustained outward current measured at the end of the voltage step ($I_{K_{SUS}}$) are shown in Fig 1D \uparrow . Note that both components of the outward K^+ current are reduced in myocytes isolated from both the left and right atria of patients in AF.

Fig 2A \downarrow shows I_{K1} traces from four different left atrial myocytes isolated from the appendages of patients in NSR at the time of surgery (top) and traces from four different left atrial myocytes isolated from the atrial appendages of patients in chronic AF (bottom). The cumulative mean \pm SEM current-voltage relations for I_{K1} in all myocytes are plotted in Fig 2B \downarrow .

Figure 2.



View larger version:
[In this page](#) [In a new window](#)
[Download as PowerPoint Slide](#)

I_{K1} density is increased in left atrial myocytes of AF patients. I_{K1} was recorded as described in the legend to Fig 1 [↑](#), at test potentials of -90 , -70 , -50 , and -30 mV. A, Currents recorded from four control myocytes are shown in the top panel; similar records from left atrial myocytes ($n=4$) isolated from chronic AF patients are shown in the lower panel. Note that the currents were normalized to cell capacitance to facilitate comparison between myocytes of different size. B,

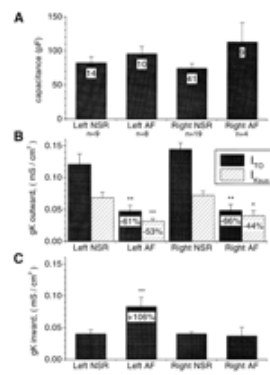
Mean \pm SEM I_{K1} density versus voltage relations are plotted for left and right NSR and AF myocytes. The number of myocytes in each group is indicated in the Fig 1 [↑](#) legend. Note that I_{K1} density is increased in the left atrial myocytes from AF patients; all other curves were indistinguishable.

The Table [↑](#) summarizes the clinical characteristics and the drug treatments of the AF patients. All but one of the patients in AF were simultaneously undergoing mitral valve repair surgery, and because of the underlying valvular disease, dilation of the left atria was obvious on visual inspection. The right atria of these patients, however, were not significantly different from those of the control patients. In an effort to discriminate between the effects of dilation and fibrillation on the K^+ currents, the electrophysiological data obtained from myocytes isolated from the left and right atrial appendages were analyzed separately.

For each myocyte, three K^+ current components were evaluated: I_{TO} , the Ca^{2+} -independent transient outward current; $I_{K_{SUS}}$, the sustained outward K^+ current; and I_{K1} , the inward rectifier K^+ current. The amplitudes of each current component in each cell were measured and normalized to cell size (capacitance). No significant differences in mean capacitance values (cell size) were evident between left and right atrial myocytes isolated from patients in NSR or in AF. There are no differences in I_{TO} or $I_{K_{SUS}}$ (Fig 3B [↓](#)) densities between myocytes isolated from the left versus the right atrial appendages of patients in NSR at the time of surgery. The densities of I_{TO} and $I_{K_{SUS}}$ were, however, significantly reduced in left and right atrial myocytes isolated from the atrial appendages of patients in AF (Fig 3B [↓](#)). In these patients, I_{TO} was reduced (compared with control values) by 61% in myocytes isolated from the left atrial appendage and by 66% in myocytes isolated from right atrial appendages. Although the density of I_{TO} was reduced, there were no significant differences in the kinetics or voltage dependences of I_{TO} activation or steady state inactivation in atrial myocytes isolated from patients in NSR compared with those isolated from patients in chronic AF. As is also evident in Fig 3B [↓](#), compared with control values, $I_{K_{SUS}}$ was reduced by 53% in the left atrial myocytes and by 44% in the right atrial myocytes obtained from patients in AF.

Figure 3.

Mean \pm SEM K^+ current densities in atrial myocytes isolated from the left and right atrial appendages of patients in chronic AF. A, Mean \pm SEM



View larger version:
[In this page](#) [In a new window](#)
[Download as PowerPoint Slide](#)

capacitance measurements for the myocytes studied in each group are displayed. The number of myocytes in each group is indicated within the bar; the source of the myocytes (ie, left and right atrial appendages of patients in NSR or AF) and the number of patients in each group are shown below each bar. There was no difference in myocyte capacitance between any of the groups. B, Mean±SEM outward K⁺ conductances (gK outward)

for I_{TO} and $I_{K_{Sus}}$ in left and right

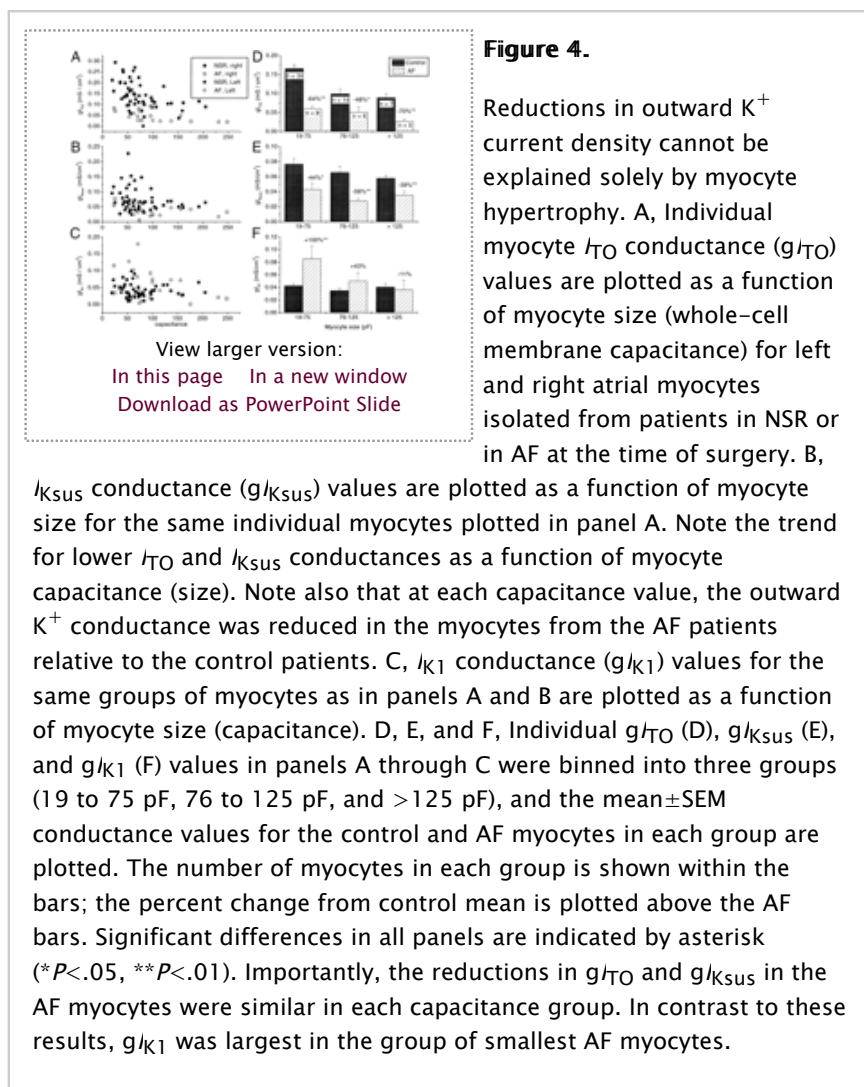
atrial myocytes from NSR and AF patients are plotted. Both I_{TO} and $I_{K_{Sus}}$ are systematically reduced in myocytes isolated from either the left or right atrial appendages of patients in chronic AF. I_{TO} and $I_{K_{Sus}}$ were determined as described in the legend of Fig 1 ↑. The percent reductions in current densities, determined relative to controls, are indicated within the bars of the AF myocyte groups. C, Inward rectifier K⁺ conductances (gK inward) were determined as the slope of the current density–voltage relationship for test potentials of –70 to –90 mV. Although I_{K1} density is not different in right atrial myocytes isolated from NSR and AF patients, there is a significant ($P<.01$) increase in I_{K1} density in left atrial myocytes from AF patients compared with NSR left atrial myocytes. The percent change from the control current density is indicated within the bar. Significant differences in all panels are indicated by asterisks (* $P<.05$, ** $P<.01$).

In contrast to the marked reductions in outward K⁺ current densities, there was a significant increase (106%) in I_{K1} density in myocytes isolated from the left atrial appendages of patients in chronic AF (Fig 3C ↑). The increased I_{K1} density results in a significantly more positive holding current (at –50 mV) in the left atrial myocytes of chronic AF patients, relative to the left atrial control myocytes ($P<.01$). Mean±SEM holding currents were $0.9±0.3$ pA ($n=10$) and $-12.7±2$ pA ($n=14$) for left atrial AF myocytes and left control myocytes, respectively. These observations suggest that resting membrane potentials may be more negative in left atrial myocytes from patients in chronic AF. No significant differences were evident, however, in I_{K1} densities or holding currents in myocytes isolated from the right atrial appendages of patients in chronic AF compared with the control patients (see “Discussion”).

Do the Observed Changes in K⁺ Current Density Simply Reflect Atrial Myocyte Hypertrophy?

Because of concerns about the impact of atrial myocyte hypertrophy (which underlies the observed atrial dilation noted above) on the density of atrial K⁺ current components, the density of each current component was evaluated as a function of cell size (whole-cell membrane capacitance). In Fig 4 ↓, the conductance values for I_{TO} (Fig 4A ↓), $I_{K_{Sus}}$ (Fig 4B ↓), and I_{K1} (Fig 4C ↓) in individual cells are plotted versus whole-cell membrane capacitance. Although there was a trend toward smaller I_{TO} and $I_{K_{Sus}}$ densities in larger myocytes, it is evident that the

densities of both outward K^+ current components were lower in the myocytes isolated from the atrial appendages of patients in AF across the entire range of capacitance values. To further evaluate the effects of hypertrophy on the measured current densities, the data from individual cell measurements were subdivided into three groups: 19 to 75 pF, 76 to 125 pF, and >125 pF. When myocytes are grouped in this way, the hypertrophy associated with AF is also evident. For example, 5 (32%) of 19 myocytes from patients in chronic AF were >125 pF, whereas only 7 (13%) of 55 myocytes from patients in NSR were in this group. Nevertheless, and as clearly illustrated in Fig 4↓, these analyses revealed that the mean reductions in I_{TO} (Fig 4D↓) and $I_{K_{sus}}$ (Fig 4E↓) densities were similar for myocytes in all three groups (19 to 75 pF, 76 to 125 pF, and >125 pF).

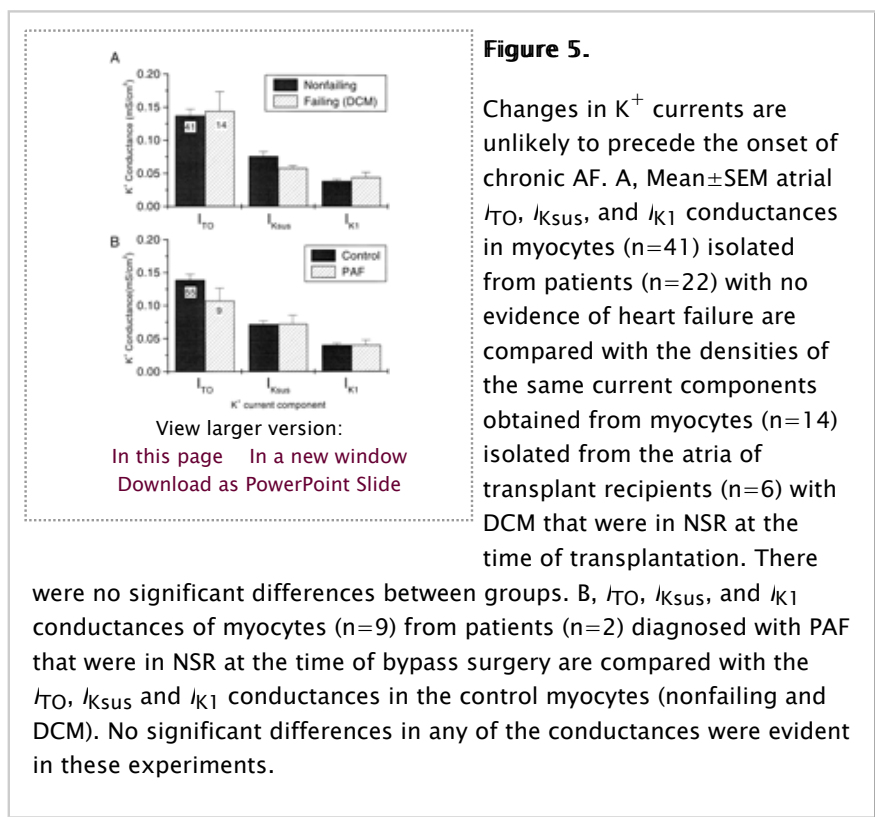


Interestingly, for I_{K_1} , the same general trend, ie, lower current density in larger myocytes, is evident (Fig 4C↑). As shown in Fig 3C↑, there was an increase in mean I_{K_1} density in the left, but not right, atrial myocytes of AF patients. When the current densities were analyzed as a function of myocyte size, it became clear that the increase in I_{K_1} density was only significant in the smallest group (19 to 75 pF) of atrial myocytes (Fig 4F↑). The significance of this observation is not clear.

Do Changes in K^+ Current Density Precede Chronic AF?

To determine whether the changes in K^+ current density occur as a result of chronic AF or whether they might be factors precipitating the rhythm disturbance,

we also evaluated K^+ current densities in two groups of patients who were in NSR at the time of surgery but who had cardiac disease and an increased risk for the development of AF. Comparison of results obtained in atrial myocytes isolated from nonfailing hearts (the nonfailing donor hearts and normal surgical patients undergoing bypass surgery) and the atrial myocytes isolated from 6 patients with end-stage heart failure (DCM) who received a heart transplant but who were in NSR at the time of transplantation revealed no significant differences in I_{TO} , $I_{K_{SUS}}$, or I_{K1} densities (Fig 5A↓). K^+ current densities were also examined in myocytes from two patients who had experienced periodic episodes of PAF but were in NSR at the time of bypass surgery. Similar to the results in Fig 5A↓, these experiments revealed no significant differences in I_{TO} , $I_{K_{SUS}}$, or I_{K1} densities in PAF myocytes compared with control myocytes (Fig 5B↓). Taken together, these results suggest that the changes in K^+ current densities described here reflect the effects of chronic AF (see “Discussion”).

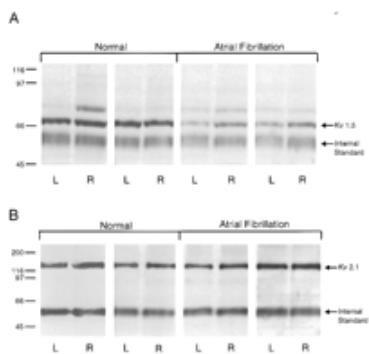


Kv1.5 Expression Is Reduced in Chronic AF

To determine if there were corresponding reductions in the expression of voltage-gated K^+ channel α -subunit proteins, Western blot analysis was performed on membrane proteins prepared from the left and right atrial appendages isolated from the same patient populations used for the electrophysiological studies. Typical Western blots with anti-Kv1.5 and anti-Kv2.1 K^+ channel α -subunit-specific antibodies are presented in Fig 6A↓ and 6B↓, respectively. To facilitate comparisons among samples and between blots, the density of the specific K^+ channel α -subunit bands was determined relative to an internal standard (rabbit IgG), as described in “Materials and Methods.”

Figure 6.

Western blots reveal that Kv1.5, but not Kv2.1, expression is decreased in the membranes of myocytes from patients in AF. Membrane proteins



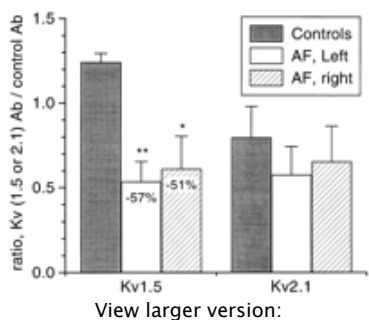
View larger version:
[In this page](#) [In a new window](#)
[Download as PowerPoint Slide](#)

were isolated from the left and right atrial appendages of patients in NSR or in chronic AF. Membrane proteins were fractionated on SDS-PAGE gels, transferred to PVDF membranes (Amersham Life Sciences), and immunoblotted with anti-Kv1.5 (A) or anti-Kv2.1 (B) antibodies. Each panel shows blots from left and right atrial appendage tissue pairs from two patients in NSR (normal) and from two patients in AF at the time of surgery. A fixed amount of

membrane protein (25 μ g) was added to each lane. Molecular weight markers are indicated on the left side of the blots. The bands labeled "internal standard" denote the position of the rabbit IgG internal standard added to each membrane protein sample. The anti-Kv1.5 antibody was used at a dilution of 1:100, and the anti-Kv2.1 antibody was used at a dilution of 1:250. Bound antibodies were detected with a chemiluminescence assay (see "Materials and Methods").

As illustrated in Fig 6 [↑](#), Kv1.5 and Kv2.1 are readily detected in membrane preparations from left and right atrial appendages of patients in NSR. Western blots of membrane proteins isolated from the left and right atrial appendages of two patients are illustrated in the left panels of Fig 6 [↑](#). The Kv1.5 and Kv2.1 bands and the internal standard are indicated. In the blot of right atrial membrane proteins from one of the patients, a prominent band at \approx 80 kD is evident. The identity of this band is not known. These figures show that the expression levels of both Kv1.5 (Fig 6A [↑](#)) and Kv2.1 (Fig 6B [↑](#)) are indistinguishable in the left and right atrial appendages of patients in NSR. Similar results were obtained in experiments completed on atrial membrane preparations from four other patients in NSR.

Western blots with the anti-Kv2.1 antibodies revealed that Kv2.1 expression in the left and right atrial appendages of two AF patients was not significantly different from that of control patients (Fig 6B [↑](#)). Quantitative analysis of the Western blots with the anti-Kv2.1-specific antibody in membrane preparations from the left and right atrial appendages of four other patients in AF confirmed these results, and mean \pm SEM normalized data are presented in Fig 7 [↓](#). For patients in AF, the mean density of Kv2.1, determined relative to the standard, from either the left (n=6) or the right (n=6) atrial appendages was not significantly different from that for the control patients (n=6).



View larger version:

Figure 7.

Densitometric analysis shows that Kv1.5, but not Kv2.1, expression levels are decreased in the membranes of patients in AF. The densities of the Kv1.5 and Kv2.1 bands were determined on Western blots such as those shown in Fig 6 [↑](#).

Quant. After background subtraction, the ratio of the density of each subunit band was normalized to the density of the internal standard (rabbit IgG) added to each sample. The mean \pm SEM relative density of the Kv1.5 and Kv2.1 α -subunit proteins in right and left atrial appendages from the AF patients (n=6) are plotted separately. Note that there is no significant difference in Kv1.5 or Kv2.1 expression levels between left and right atrial appendages from AF patients. In both left and right appendages, Kv1.5 expression is decreased; Kv2.1, however, is unaffected. Statistically significant changes are marked with asterisks (* P <.05, ** P <.01). The percent change from control is indicated within the bar.

In contrast to the results with Kv2.1, Kv1.5 expression levels were clearly reduced in membranes prepared from the left and right atrial appendages of patients in AF (Fig 6A \uparrow). Similar to the control hearts, however, there is no significant difference in Kv1.5 expression between the left and right atrial appendages from AF patients. Western blots of membrane proteins from the atrial appendages of two AF patients are displayed in the right panels of Fig 6A \uparrow . Similar results were also obtained in Western blots performed on atrial appendage membrane preparations from four other AF patients. Kv1.5 densities were determined in all samples and normalized to the internal IgG standard; mean \pm SEM normalized data are presented in Fig 7 \uparrow . The mean density of Kv1.5 was reduced by 57% in the left atrial appendages (n=6) and by 51% in the right atrial appendages (n=6) of patients in chronic AF.

Discussion

Outward K⁺ Currents Are Reduced in Chronic AF

In the chronic model of AF developed in goats by Allessie and colleagues,^{4 18} it was demonstrated that induction of AF for extended periods was directly responsible for the increased duration of subsequent episodes of fibrillation. In addition, within 1 week of pacing-induced fibrillation, AF was self-sustained in 10 of 11 animals. Over this 1-week period, the action potential duration and effective refractory period were decreased, and the median activation interval (F-F) was also reduced. The observed changes in all of these parameters were statistically significant and were fully reversible upon cardioversion and removal of the external pacing stimulus. These results led the authors to suggest that rapid electrophysiological remodeling occurs in AF as a direct result of the fibrillatory process. Recent studies in patients have shown that a rapid reduction in atrial effective refractory period is also associated with the initiation of AF in humans.²

Because the reductions in refractory period and action potential duration are associated with the onset and maintenance of chronic AF, we hypothesized that outward K⁺ current densities would be increased in atrial myocytes isolated from patients in chronic AF compared with myocytes isolated from patients in NSR. However, the results presented here clearly demonstrate that this hypothesis is incorrect. Rather, our results demonstrate that I_{TO} and $I_{K_{sus}}$ densities are significantly reduced in myocytes isolated from both the left and right atrial appendages of patients in chronic AF.

By comparing the K⁺ current densities of patients at increased risk for the development of chronic AF with normal patients, we have attempted to determine

whether the observed reduction in K^+ current density in patients with chronic AF is a result of the disease process or a pathological change that precedes the onset of chronic AF. As demonstrated in Fig 5 [↑](#), there was no significant difference in any of the K^+ current densities in myocytes isolated from patients with either DCM or PAF relative to myocytes isolated from control patients. Importantly, from a clinical perspective, both groups are at a significant risk for the development of chronic AF. Thus, our results strongly suggest that it is the chronic AF, per se, that causes the reduction in outward K^+ current densities.

Effects of AF on Atrial K^+ Currents Are Not Due to Atrial Dilation or Hypertrophy

In the AF patient population studied here, substantial left atrial dilation was present in nearly all of the AF patients (Table [↑](#)), whereas there was no significant right atrial enlargement in most of these patients. Le Grand et al¹⁹ demonstrated that outward K^+ current densities were reduced in myocytes isolated from dilated (but not necessarily fibrillating) atria. In the present study, it is evident (Fig 4 [↑](#)) that an increase in atrial myocyte size (capacitance) is correlated with a decreased density of all K^+ current (I_{TO} , $I_{K_{Sus}}$, and I_{K1}) components examined. However, we note that I_{TO} and $I_{K_{Sus}}$ densities were reduced to a similar degree in myocytes isolated from both the dilated left and normal-sized right atrial appendages. In addition, significant reductions in I_{TO} and $I_{K_{Sus}}$ densities were evident in all AF myocytes, regardless of cell size (Fig 4 [↑](#)). Taken together, these results suggest that significant reductions in I_{TO} and $I_{K_{Sus}}$ are a direct result of chronic AF, per se, and are not simply the result of atrial dilation and/or increase in myocyte size. Thus, it seems apparent that chronic AF, in the absence of visually or echocardiographically evident atrial dilation, is associated with a reduction in outward K^+ current density similar to or greater than that caused by atrial dilation alone.

Interestingly, the reduction in I_{K1} density with increased myocyte size (capacitance) appears to be attenuated in left atrial myocytes isolated from patients in chronic AF. On average, I_{K1} density was 106% greater in left atrial myocytes from fibrillating atria ($P < .01$), whereas there was no significant difference in I_{K1} density in myocytes isolated from the right atrial appendages of patients in AF compared with those isolated from patients in NSR. An increased I_{K1} density may result in more negative resting potentials and earlier repolarization in the left atrial myocytes of chronic AF patients. To better understand the significance of this observation, further experiments aimed at determining and comparing resting membrane potentials and Ba^{2+} -sensitive I_{K1} current densities in atrial myocytes isolated from both normal and chronic AF patients are warranted.

AF Is Associated With a Reduced Expression of Kv1.5, But Not Kv2.1, α Subunits

Western blot analysis of Kv2.1 α -subunit expression in atrial appendages from control patients in NSR and from patients in chronic AF revealed that there was no significant difference in the expression of Kv2.1 between these two patient groups. This observation suggests that the observed reduction in $I_{K_{Sus}}$ is not due to a loss of K^+ channels containing Kv2.1 α subunits. The simplest interpretation of these results is that Kv2.1 α subunits may not contribute importantly to the outward K^+ currents in isolated human atrial myocytes. In support of this hypothesis, we have found that very little tetraethylammonium-sensitive current is apparent in human atrial myocytes (authors' unpublished observation, 1996). The currents produced by heterologous expression of Kv2.1, however, are tetraethylammonium sensitive.²⁰

It has been shown that I_{Kur} is a primary component of the human atrial delayed rectifier K^+ current,²¹ and it has been suggested that Kv1.5 underlies this current.⁷ Consistent with the latter hypothesis, recent immunohistochemical studies have also demonstrated Kv1.5 protein expression in human atrium.¹⁰ Previous studies in other preparations have also shown that the expression of Kv1.5 can be modulated by a variety of influences, including glucocorticoids,²² thyrotropin-releasing hormone,¹⁶ and, intriguingly, membrane depolarization.²³ Elevated extracellular K^+ (50 mmol/L), for example, specifically suppressed Kv1.5 (but not Kv1.4 or Kv2.1) expression in cultured GH₃ cells.²³ These results were interpreted as suggesting that variations in membrane potential (or any changes in electrical activity) can regulate Kv1.5 expression.²³

The results presented here demonstrate that Kv1.5 expression is also reduced in the atria of patients in AF, by 57% and 51% in the left and right atrial appendages, respectively. Interestingly, these values closely parallel the reductions in $I_{K_{Sus}}$ of 53% and 44% in the myocytes isolated from the left and right atrial appendages, respectively, of patients in AF. Thus, the decrement in $I_{K_{Sus}}$ closely paralleled the reduction of Kv1.5 expression. This close correlation between the reduction in delayed rectifier K^+ current density and the reduction in Kv1.5 expression supports the hypothesis that the Kv1.5 α subunit contributes importantly to the delayed rectifier K^+ current in human atria.⁷

The activation interval (FF interval, or the interval between subsequent activations of the atria) is substantially reduced in the fibrillating atria (typically <200 milliseconds²⁴ versus 600 to 800 milliseconds [normal]). Thus, atrial myocytes from the fibrillating atria must be in a depolarized state for a greater fraction of the time. Indeed, monophasic action potential recordings from patients in AF frequently demonstrate incomplete repolarization.²⁵ It seems reasonable to speculate, therefore, that the downregulation of Kv1.5 expression observed here results from the altered electrical activity of the atrium.

Effects of AF on Other K^+ Currents

Even if the hypothesis that Kv1.5 underlies I_{Kur} is correct,⁷ it is clear that there are other currents that contribute to the total outward K^+ currents in human atrial myocytes. I_{Kr} , for example, has been documented in human atrial myocytes.²⁶ Importantly, this current is the target of all presently approved class III antiarrhythmic drugs. *H-erg* has recently been identified as the genetic locus of long QT2²⁷ and has been shown in heterologous expression systems to produce currents that closely resemble I_{Kr} ,^{27 28} suggesting that *H-erg* underlies I_{Kr} . It will be of interest, therefore, to determine if I_{Kr} densities and *H-erg* expression are also affected by AF. Clearly, such studies will require the availability of specific anti-*H-erg* antibodies.

The results presented here also revealed that the density of I_{TO} is significantly reduced in human atrial myocytes isolated from patients in AF compared with age-matched control patients in NSR (Figs 1 through 4 $\uparrow\uparrow\uparrow\uparrow$). Recent studies have demonstrated that Kv4.3 message levels are high in the human ventricle, leading to the suggestion that Kv4.3 is a likely α subunit contributing to I_{TO} in the human heart.²⁹ Further studies, aimed at confirming the presence of the Kv4.3 protein in human atria and at examining the impact of AF on the expression of this subunit, are clearly warranted. These experiments will require the availability of specific (anti-Kv4.3) antibodies.

Implicit Role for a Reduction in Inward Ca^{2+} Current Density

In the studies of Le Grand et al¹⁹ on electrophysiological changes in dilated human atria, a greater reduction in Ca^{2+} current density was detected (75%) relative to the reduction in outward K^{+} current density (60%). Changes in Ca^{2+} current density could likely explain the shortenings in action potential duration and effective refractory period that are observed during chronic AF. Interestingly, Ca^{2+} channel blockers have been found to prevent both the changes in effective refractory period³⁰ and contractile dysfunction³¹ that accompany short episodes of AF. This strongly suggests that Ca^{2+} overload may be the proximal mechanism initiating both the changes in Ca^{2+} current density and the eventual reduction in K^{+} current density. Intriguingly, although we have shown that there was no difference in K^{+} current density between our control atrial myocytes isolated from nonfailing hearts and those isolated from the explanted hearts of transplant recipients in NSR with DCM, Ouadid et al³² demonstrated that atrial myocytes from transplant recipients had significantly lower peak Ca^{2+} current densities (2 ± 1 pA/pF) than did myocytes isolated from a control population of bypass patients (12 ± 4 pA/pF). Because patients in heart failure have an increased incidence of AF, the present study supports the hypothesis that a reduction in Ca^{2+} current density may be involved in the initiation and/or maintenance of chronic AF. Clearly, studies focused on examining human atrial myocyte Ca^{2+} current densities and Ca^{2+} channel expression in patients with chronic AF and in patients predisposed to develop AF would be of great interest.

Summary

AF is a complex multifaceted disorder. Although sometimes tolerated for long periods, AF causes substantial discomfort and significantly increases the risk of thromboembolic events. Although AF can be induced briefly even in normal patients, there are clear decreases in refractory period with sustained episodes of AF.² These long-term changes in refractory period are likely to reflect the fibrillation-induced changes in the expression of atrial ion channels. The present study has shown that chronic AF is associated with a decreased outward K^{+} current density and a reduced expression of Kv1.5 α subunits. Our results suggest that these changes are the result, rather than the cause, of the chronic AF.

Drugs that block K^{+} channels (eg, sotalol, dofetilide, ibutilide) are now commonly used to treat patients in AF. Clinical studies have shown that these drugs are most effective in treating patients with recent onset AF (days to weeks). The present study suggests that this loss of efficacy may in part be explained by the overall reduction in outward K^{+} current, since an incremental suppression of a small repolarizing current may be less effective than when normal densities of repolarizing currents are present. Further studies aimed at identifying the components of the outward atrial K^{+} current that are reduced and the specific K^{+} channel subunits that are modulated by the presence of AF are also clearly warranted. Once this information is available, it may be possible to develop new therapeutic strategies for the treatment of AF that have fewer side effects than currently available therapies.

Selected Abbreviations and Acronyms

AF =atrial fibrillation
BDM =butanedione monoxime
DCM =dilated cardiomyopathy
 I_{K1} =inward rectifier K^{+} current
 I_{Kr} , =rapid and slow components of
 I_{Ks} delayed rectifier K^{+} current
 I_{Ksus} =sustained outward K^{+} current

I_{Kur} =ultrarapid delayed rectifier K^+ current
 I_{TO} =transient outward K^+ current
NSR =normal sinus rhythm
PAF =paroxysmal AF

Acknowledgments

This study was supported by grants from Procter and Gamble Pharmaceuticals (Dr Van Wagoner), the National Institutes of Health (Dr Nerbonne), and the Monsanto/Searle/Washington University Biomedical Research Program (Dr Nerbonne). This work was done during the tenure of an Established Investigatorship from the American Heart Association (Dr Trimmer). Thanks are extended to Peggy Kirian and Michelle Lamorgese for expert technical assistance. We gratefully acknowledge the efforts of Dr Robert W. Stewart and Dr Christine Moravec for coordinating the Research Transplant Team, as well as the assistance of Dr Delos Cosgrove, for providing generous access to surgical tissue.

Received June 21, 1996.

Accepted March 21, 1997.

© 1997 American Heart Association, Inc.

References

1. Alnert IS, Petersen P, Godtfredsen I. Atrial fibrillation: natural history, complications and management. *Annu Rev Med.* 1988;39:41-52. [CrossRef](#)
[Medline](#)
2. Daoud FO, Roguin F, Coval R, Harvey M, Man KC, Strickberger A, Morady F. Effect of atrial fibrillation on atrial refractoriness in humans. *Circulation.* 1996;94:1600-1606. [Abstract/FREE Full Text](#)
3. Routidir M, Le Henvez IY, Lavergne T, Chauvaud S, Guize L, Carpentier A, Baronnat B. Inhomogeneity of cellular refractoriness in human atrium: factor of arrhythmia? *Pacing Clin Electrophysiol.* 1986;9:1095-1100. [CrossRef](#)
[Medline](#)
4. Wiiffels MCFE, Kirchof CHH, Dorland RD, Alessie MA. Atrial fibrillation begets atrial fibrillation: a study in awake chronically instrumented goats. *Circulation.* 1995;92:1954-1968. [Abstract/FREE Full Text](#)
5. Escande D, Coulombe A, Faivre IF, Deroubaix F, Corahoeuf F. Two types of transient outward currents in adult human atrial cells. *Am J Physiol.* 1987;252:H142-H148. [Abstract/FREE Full Text](#)
6. Fermini R, Wang Z, Duan D, Nattel S. Differences in rate dependence of transient outward current in rabbit and human atrium. *Am J Physiol.* 1992;263:H1747-H1754. [Abstract/FREE Full Text](#)
7. Fedida D, Wible R, Wang Z, Fermini R, Faust F, Nattel S, Brown AM. Identity of a novel delayed rectifier current from human heart with a cloned K^+ channel current. *Circ Res.* 1993;73:210-216. [Abstract/FREE Full Text](#)
8. Wang Z, Fermini R, Nattel S. Delayed rectifier outward current and repolarization in human atrial myocytes. *Circ Res.* 1993;73:276-285. [Abstract/FREE Full Text](#)
9. Roberds SL, Tamkun MM. Cloning and tissue-specific expression of five voltage-gated potassium channel cDNAs expressed in rat heart. *Proc Natl Acad Sci U S A.* 1991;88:1798-1802. [Abstract/FREE Full Text](#)
10. Mays DL, Foose IM, Philinson LH, Tamkun MM. Localization of the Kv1.5 K^+ channel protein in explanted cardiac tissue. *J Clin Invest.* 1995;96:282-292.

11. McCarthy PM, Castle LW, Maloney JD, Trohman RC, Simmons TW, White RD, Klein AL, Cosgrove DM. Initial experience with the Maze procedure for atrial fibrillation. *J Thorac Cardiovasc Surg.* 1995;105:1077-1087. [Medline](#)
12. Cox JL, Boineau JP, Schuessler RB, Kater KM, Ferguson TB, Cain ME, Lindsay BD, Smith IM, Corr PB, Hoque CB, Lappas DG. Electrophysiological basis, surgical development, and clinical results of the Maze procedure for atrial flutter and atrial fibrillation. *Adv Card Surg.* 1995;6:1-67. [Medline](#)
13. Korn SI, Horn R. Influence of sodium-calcium exchange on calcium current rundown and the duration of calcium-dependent chloride currents in pituitary cells: studied with whole-cell and perforated-patch recording. *J Gen Physiol.* 1989;94:789-812. [Abstract/FREE Full Text](#)
14. Van Wagoner DR, Kirian M, Lamorgese M. Phenylephrine suppresses outward K^+ currents in rat atrial myocytes. *Am J Physiol.* 1996;271:H937-H946. [Abstract/FREE Full Text](#)
15. Barry DM, Trimmer IS, Merlie JP, Nerbonne JM. Differential expression of voltage-gated K^+ channel subunits in adult rat heart: relation to functional K^+ channels? *Circ Res.* 1995;77:361-369. [Abstract/FREE Full Text](#)
16. Takimoto K, Gealy R, Fomina AF, Trimmer IS, Levitan ES. Inhibition of voltage-gated K^+ channel gene expression by the neuropeptide thyrotropin-releasing hormone. *J Neurosci.* 1995;15:449-457. [Abstract](#)
17. Trimmer IS. Immunological identification and characterization of a delayed rectifier K^+ channel polypeptide in rat brain. *Proc Natl Acad Sci U S A.* 1991;88:10764-10768. [Abstract/FREE Full Text](#)
18. Allessie MA, Wiiffels MCFE, Kirchhof CIHJ. Experimental models of arrhythmias: toys or truth? *Eur Heart J.* 1994;15:2-8. [FREE Full Text](#)
19. Le Grand R, Hatem S, Deroubaix F, Couétil I-P, Coraboeuf E. Depressed transient outward and calcium currents in dilated human atria. *Cardiovasc Res.* 1994;28:548-556. [Medline](#)
20. Alhrecht B, Lorra C, Stocker M, Pongs O. Cloning and characterization of a human delayed rectifier potassium channel gene. *Recept Channels.* 1993;1:99-110. [Medline](#)
21. Wang Z, Fermini B, Nattel S. Sustained depolarization-induced outward current in human atrial myocytes: evidence for a novel delayed rectifier K^+ current similar to Kv1.5 cloned channel currents. *Circ Res.* 1993;73:1061-1076. [Abstract/FREE Full Text](#)
22. Takimoto K, Levitan ES. Glucocorticoid induction of Kv1.5 K^+ channel gene expression in ventricle of rat heart. *Circ Res.* 1994;75:1006-1013. [Abstract/FREE Full Text](#)
23. Levitan ES, Gealy R, Trimmer IS, Takimoto K. Membrane depolarization inhibits Kv1.5 voltage-gated K^+ channel gene transcription and protein expression in pituitary cells. *J Biol Chem.* 1995;270:6036-6041. [Abstract/FREE Full Text](#)
24. Capucci A, Riffi M, Boriana G, Ravelli F, Nollo G, Sabbatini P, Orsi C, Magnani R. Dynamic electrophysiological behavior of human atria during paroxysmal atrial fibrillation. *Circulation.* 1995;92:1193-1202. [Abstract/FREE Full Text](#)
25. Olsson SB, Cai N, Edvardsson N, Talwar KK. Prediction of terminal atrial myocardial repolarization from incomplete phase 3 data. *Cardiovasc Res.* 1989;23:53-59. [Medline](#)
26. Wang Z, Fermini B, Nattel S. Rapid and slow components of delayed rectifier current in human atrial myocytes. *Cardiovasc Res.* 1995;28:1540-1546. [CrossRef](#)

27. Sanquinetti MC, Liang C, Curran ME, Keating MT. A mechanistic link between an inherited and an acquired cardiac arrhythmia: HERG encodes the I_{Kr} potassium channel. *Cell*. 1995;81:299–307. [CrossRef](#) [Medline](#)
28. Trudeau MC, Warmke LW, Ganetzky R, Robertson GA. HERG, a human inward rectifier in the voltage-gated potassium channel family. *Science*. 1995;269:92–95. [Abstract/FREE Full Text](#)
29. Dixon JF, Shi W, Wang H-S, McDonald C, Yu H, Wymore RS, Cohen IS, McKinnon D. Role of the $Kv4.3$ K^+ channel in ventricular muscle: a molecular correlate for the transient outward current. *Circ Res*. 1996;79:659–668. [Abstract/FREE Full Text](#)
30. Goette A, Honeycutt C, Langberg H. Electrical remodeling in atrial fibrillation: time course and mechanisms. *Circulation*. 1996;94:2968–2974. [Abstract/FREE Full Text](#)
31. Laistad F, Aksnes G, Verburg F, Christensen G. Atrial contractile dysfunction after short-term atrial fibrillation is reduced by verapamil but increased by Bay K 8644. *Circulation*. 1996;93:1747–1754. [Abstract/FREE Full Text](#)
32. Quadid H, Alhat R, Nargeot I. Calcium currents in diseased human cardiac cells. *J Cardiovasc Pharmacol*. 1995;25:282–291. [Medline](#)

Articles citing this article

Down-regulation of the Small Conductance Calcium-activated Potassium Channels in Diabetic Mouse Atria

J Biol Chem. 2015;290:7016–7026,

[Abstract](#) [Full Text](#) [PDF](#)

Left Atrial Transcriptional Changes Associated With Atrial Fibrillation Susceptibility and Persistence

Circ Arrhythm Electrophysiol. 2015;8:32–41,

[Abstract](#) [Full Text](#) [PDF](#)

Reduced Sialylation Impacts Ventricular Repolarization by Modulating Specific K^+ Channel Isoforms Distinctly

J Biol Chem. 2015;290:2769–2783,

[Abstract](#) [Full Text](#) [PDF](#)

TASK-1 current is inhibited by phosphorylation during human and canine chronic atrial fibrillation

Am. J. Physiol. Heart Circ. Physiol.. 2015;308:H126–H134,

[Abstract](#) [Full Text](#) [PDF](#)

Cellular and Molecular Electrophysiology of Atrial Fibrillation Initiation, Maintenance, and Progression

Circ. Res.. 2014;114:1483–1499,

[Abstract](#) [Full Text](#) [PDF](#)

Mathematical Approaches to Understanding and Imaging Atrial Fibrillation: Significance for Mechanisms and Management

Circ. Res.. 2014;114:1516–1531,

[Abstract](#) [Full Text](#) [PDF](#)

Cardiac Potassium Channel Subtypes: New Roles in Repolarization and Arrhythmia

Physiol. Rev.. 2014;94:609–653,

[Abstract](#) | [Full Text](#) | [PDF](#)

Role for Myosin-V Motor Proteins in the Selective Delivery of Kv Channel Isoforms to the Membrane Surface of Cardiac Myocytes

Circ. Res.. 2014;114:982–992,

[Abstract](#) | [Full Text](#) | [PDF](#)

Multi-channel blockers for treatment of atrial fibrillation: an effective strategy?

Cardiovasc Res. 2013;98:5–6,

[Full Text](#) | [PDF](#)

Rotors and the Dynamics of Cardiac Fibrillation

Circ. Res.. 2013;112:849–862,

[Abstract](#) | [Full Text](#) | [PDF](#)

Chronic atrial fibrillation up-regulates β 1-Adrenoceptors affecting repolarizing currents and action potential duration

Cardiovasc Res. 2013;97:379–388,

[Abstract](#) | [Full Text](#) | [PDF](#)

Translational Research in Atrial Fibrillation: A Quest for Mechanistically Based Diagnosis and Therapy

Circ Arrhythm Electrophysiol. 2012;5:1207–1215,

[Full Text](#) | [PDF](#)

Cellular and molecular correlates of ectopic activity in patients with atrial fibrillation

Europace. 2012;14:v97–v105,

[Abstract](#) | [Full Text](#) | [PDF](#)

The role of action potential alternans in the initiation of atrial fibrillation in humans: a review and future directions

Europace. 2012;14:v58–v64,

[Abstract](#) | [Full Text](#) | [PDF](#)

Redox-Sensitive Sulfenic Acid Modification Regulates Surface Expression of the Cardiovascular Voltage-Gated Potassium Channel Kv1.5

Circ. Res.. 2012;111:842–853,

[Abstract](#) | [Full Text](#) | [PDF](#)

Ablation of sarcolipin results in atrial remodeling

Am. J. Physiol. Cell Physiol.. 2012;302:C1762–C1771,

[Abstract](#) | [Full Text](#) | [PDF](#)

Enhanced Sarcoplasmic Reticulum Ca²⁺ Leak and Increased

Na⁺-Ca²⁺ Exchanger Function Underlie Delayed Afterdepolarizations in Patients With Chronic Atrial Fibrillation

Circulation. 2012;125:2059-2070,

[Abstract](#) | [Full Text](#) | [PDF](#)

Rate-Dependent Effects of Vernakalant in the Isolated Non-Remodeled Canine Left Atria Are Primarily Due to Block of the Sodium Channel: Comparison With Ranolazine and dl-Sotalol

Circ Arrhythm Electrophysiol. 2012;5:400-408,

[Abstract](#) | [Full Text](#) | [PDF](#)

The Na⁺/K⁺ pump is an important modulator of refractoriness and rotor dynamics in human atrial tissue

Am. J. Physiol. Heart Circ. Physiol.. 2012;302:H1146-H1159,

[Abstract](#) | [Full Text](#) | [PDF](#)

Differential Protein Kinase C Isoform Regulation and Increased Constitutive Activity of Acetylcholine-Regulated Potassium Channels in Atrial Remodeling

Circ. Res.. 2011;109:1031-1043,

[Abstract](#) | [Full Text](#) | [PDF](#)

Cortactin Is Required for N-cadherin Regulation of Kv1.5 Channel Function

J Biol Chem. 2011;286:20478-20489,

[Abstract](#) | [Full Text](#) | [PDF](#)

Monogenic atrial fibrillation as pathophysiological paradigms

Cardiovasc Res. 2011;89:692-700,

[Abstract](#) | [Full Text](#) | [PDF](#)

Alterations of atrial Ca²⁺ handling as cause and consequence of atrial fibrillation

Cardiovasc Res. 2011;89:722-733,

[Abstract](#) | [Full Text](#) | [PDF](#)

Ultra-rapid delayed rectifier channels: molecular basis and therapeutic implications

Cardiovasc Res. 2011;89:776-785,

[Abstract](#) | [Full Text](#) | [PDF](#)

MicroRNAs and atrial fibrillation: new fundamentals

Cardiovasc Res. 2011;89:710-721,

[Abstract](#) | [Full Text](#) | [PDF](#)

Time course and mechanisms of endo-epicardial electrical dissociation during atrial fibrillation in the goat

Cardiovasc Res. 2011;89:816-824,

[Abstract](#) | [Full Text](#) | [PDF](#)

Pathophysiological Mechanisms of Atrial Fibrillation: A Translational

Appraisal

Physiol. Rev.. 2011;91:265–325,

[Abstract](#) | [Full Text](#) | [PDF](#)

Left-to-Right Atrial Inward Rectifier Potassium Current Gradients in Patients With Paroxysmal Versus Chronic Atrial Fibrillation

Circ Arrhythm Electrophysiol. 2010;3:472–480,

[Abstract](#) | [Full Text](#) | [PDF](#)

Chronic heart failure and the substrate for atrial fibrillation

Cardiovasc Res. 2009;84:227–236,

[Abstract](#) | [Full Text](#) | [PDF](#)

Effects of Potassium Channel Blockers on Changes in Refractoriness of Atrial Cardiomyocytes Induced by Stretch

Exp Biol Med (Maywood). 2009;234:779–784,

[Abstract](#) | [Full Text](#) | [PDF](#)

Funny Current Downregulation and Sinus Node Dysfunction Associated With Atrial Tachyarrhythmia: A Molecular Basis for Tachycardia–Bradycardia Syndrome

Circulation. 2009;119:1576–1585,

[Abstract](#) | [Full Text](#) | [PDF](#)

Remodelling of cardiac repolarization: how homeostatic responses can lead to arrhythmogenesis

Cardiovasc Res. 2009;81:491–499,

[Abstract](#) | [Full Text](#) | [PDF](#)

Omega–3 polyunsaturated fatty acids inhibit transient outward and ultra–rapid delayed rectifier K⁺ currents and Na⁺ current in human atrial myocytes

Cardiovasc Res. 2009;81:286–293,

[Abstract](#) | [Full Text](#) | [PDF](#)

Shared requirement for dynein function and intact microtubule cytoskeleton for normal surface expression of cardiac potassium channels

Am. J. Physiol. Heart Circ. Physiol.. 2009;296:H71–H83,

[Abstract](#) | [Full Text](#) | [PDF](#)

Inhibition of the renin–angiotensin system: effects on tachycardia–induced early electrical remodelling in rabbit atrium

Journal of Renin–Angiotensin–Aldosterone System. 2008;9:125–132,

[Abstract](#) | [PDF](#)

Four and a half LIM protein 1: a partner for KCNA5 in human atrium

Cardiovasc Res. 2008;78:449–457,

[Abstract](#) | [Full Text](#) | [PDF](#)

Review: Atrial fibrillation and renin–angiotensin system

Ther Adv Cardiovasc Dis. 2008;2:215–223,

[Abstract](#) | [PDF](#)

The anchoring protein SAP97 retains Kv1.5 channels in the plasma membrane of cardiac myocytes

Am. J. Physiol. Heart Circ. Physiol.. 2008;294:H1851–H1861,

[Abstract](#) | [Full Text](#) | [PDF](#)

Caveolin Regulates Kv1.5 Trafficking to Cholesterol-Rich Membrane Microdomains

Mol. Pharmacol.. 2008;73:678–685,

[Abstract](#) | [Full Text](#) | [PDF](#)

In silico study on the effects of IKur block kinetics on prolongation of human action potential after atrial fibrillation-induced electrical remodeling

Am. J. Physiol. Heart Circ. Physiol.. 2008;294:H793–H800,

[Abstract](#) | [Full Text](#) | [PDF](#)

Changes in IK,ACh single-channel activity with atrial tachycardia remodelling in canine atrial cardiomyocytes

Cardiovasc Res. 2008;77:35–43,

[Abstract](#) | [Full Text](#) | [PDF](#)

Localization and mobility of the delayed-rectifier K⁺ channel Kv2.1 in adult cardiomyocytes

Am. J. Physiol. Heart Circ. Physiol.. 2008;294:H229–H237,

[Abstract](#) | [Full Text](#) | [PDF](#)

Localization and trafficking of cardiac voltage-gated potassium channels

Biochim. Soc. Trans.. 2007;35:1069–1073,

[Abstract](#) | [Full Text](#) | [PDF](#)

Rab-GTPase-dependent Endocytic Recycling of KV1.5 in Atrial Myocytes

J Biol Chem. 2007;282:29612–29620,

[Abstract](#) | [Full Text](#) | [PDF](#)

Differential phosphorylation-dependent regulation of constitutively active and muscarinic receptor-activated IK,ACh channels in patients with chronic atrial fibrillation

Cardiovasc Res. 2007;74:426–437,

[Abstract](#) | [Full Text](#) | [PDF](#)

Losartan prevents stretch-induced electrical remodeling in cultured atrial neonatal myocytes

Am. J. Physiol. Heart Circ. Physiol.. 2007;292:H2898–H2905,

[Abstract](#) | [Full Text](#) | [PDF](#)

Arrhythmogenic Ion-Channel Remodeling in the Heart: Heart Failure,

Myocardial Infarction, and Atrial Fibrillation

Physiol. Rev.. 2007;87:425-456,

[Abstract](#) | [Full Text](#) | [PDF](#)

Increased Susceptibility to Atrial Tachyarrhythmia in Spontaneously Hypertensive Rat Hearts

Hypertension. 2007;49:498-505,

[Abstract](#) | [Full Text](#) | [PDF](#)

Familial clustering of lone atrial fibrillation in patients with saddleback-type ST-segment elevation in right precordial leads

Eur Heart J. 2007;28:463-468,

[Abstract](#) | [Full Text](#) | [PDF](#)

Blockade of atrial-specific K⁺-currents increases atrial but not ventricular contractility by enhancing reverse mode Na⁺/Ca²⁺-exchange

Cardiovasc Res. 2007;73:37-47,

[Abstract](#) | [Full Text](#) | [PDF](#)

Atrial fibrillation: Is NO an answer for refractoriness?

Cardiovasc Res. 2006;72:7-8,

[Full Text](#) | [PDF](#)

AVE0118, Blocker of the Transient Outward Current (I_{to}) and Ultrarapid Delayed Rectifier Current (I_{Kur}), Fully Restores Atrial Contractility After Cardioversion of Atrial Fibrillation in the Goat

Circulation. 2006;114:1234-1242,

[Abstract](#) | [Full Text](#) | [PDF](#)

Kv1.5 channelopathy due to KCNA5 loss-of-function mutation causes human atrial fibrillation

Hum Mol Genet. 2006;15:2185-2191,

[Abstract](#) | [Full Text](#) | [PDF](#)

Differential autocrine modulation of atrial and ventricular potassium currents and of oxidative stress in diabetic rats

Am. J. Physiol. Heart Circ. Physiol.. 2006;290:H1879-H1888,

[Abstract](#) | [Full Text](#) | [PDF](#)

Kir3-Based Inward Rectifier Potassium Current: Potential Role in Atrial Tachycardia Remodeling Effects on Atrial Repolarization and Arrhythmias

Circulation. 2006;113:1730-1737,

[Abstract](#) | [Full Text](#) | [PDF](#)

The G Protein-Gated Potassium Current I_{K,ACh} Is Constitutively Active in Patients With Chronic Atrial Fibrillation

Circulation. 2005;112:3697-3706,

[Abstract](#) | [Full Text](#) | [PDF](#)

Molecular Basis of Arrhythmias

Circulation. 2005;112:2517-2529,

[Abstract](#) | [Full Text](#) | [PDF](#)

Effects of hyperthyroidism on delayed rectifier K⁺ currents in left and right murine atria

Am. J. Physiol. Heart Circ. Physiol.. 2005;289:H1448-H1455,

[Abstract](#) | [Full Text](#) | [PDF](#)

Molecular Physiology of Cardiac Repolarization

Physiol. Rev.. 2005;85:1205-1253,

[Abstract](#) | [Full Text](#) | [PDF](#)

Kv1.5 Surface Expression Is Modulated by Retrograde Trafficking of Newly Endocytosed Channels by the Dynein Motor

Circ. Res.. 2005;97:363-371,

[Abstract](#) | [Full Text](#) | [PDF](#)

Human Atrial Ion Channel and Transporter Subunit Gene-Expression Remodeling Associated With Valvular Heart Disease and Atrial Fibrillation

Circulation. 2005;112:471-481,

[Abstract](#) | [Full Text](#) | [PDF](#)

Consequences of atrial electrical remodeling for the anti-arrhythmic action of class IC and class III drugs

Cardiovasc Res. 2005;67:69-76,

[Abstract](#) | [Full Text](#) | [PDF](#)

Role of up-regulation of IK1 in action potential shortening associated with atrial fibrillation in humans

Cardiovasc Res. 2005;66:493-502,

[Abstract](#) | [Full Text](#) | [PDF](#)

Ventricularization of Atrial Gene Expression in the Fibrillating Heart?

Circ. Res.. 2005;96:923-924,

[Full Text](#) | [PDF](#)

Role of IKur in Controlling Action Potential Shape and Contractility in the Human Atrium: Influence of Chronic Atrial Fibrillation

Circulation. 2004;110:2299-2306,

[Abstract](#) | [Full Text](#) | [PDF](#)

"Early" Class III Drugs for the Treatment of Atrial Fibrillation: Efficacy and Atrial Selectivity of AVE0118 in Remodeled Atria of the Goat

Circulation. 2004;110:1717-1724,

[Abstract](#) | [Full Text](#) | [PDF](#)

Atrial Ionic Remodeling Induced by Atrial Tachycardia in the Presence of Congestive Heart Failure

Circulation. 2004;110:1520–1526,

[Abstract](#) | [Full Text](#) | [PDF](#)

Atrial Fibrillation Is Associated With Increased Spontaneous Calcium Release From the Sarcoplasmic Reticulum in Human Atrial Myocytes

Circulation. 2004;110:1358–1363,

[Abstract](#) | [Full Text](#) | [PDF](#)

Atrial natriuretic peptide modulates the hyperpolarization–activated current (I_f) in human atrial myocytes

Cardiovasc Res. 2004;63:528–536,

[Abstract](#) | [Full Text](#) | [PDF](#)

Structure and Function of Kv4–Family Transient Potassium Channels

Physiol. Rev.. 2004;84:803–833,

[Abstract](#) | [Full Text](#) | [PDF](#)

Electrotonic load triggers remodeling of repolarizing current I_{to} in ventricle

Am. J. Physiol. Heart Circ. Physiol.. 2004;286:H1901–H1909,

[Abstract](#) | [Full Text](#) | [PDF](#)

Current Perspectives of Electrical Remodeling and Its Therapeutic Implications

J CARDIOVASC PHARMACOL THER. 2004;9:129–144,

[Abstract](#) | [PDF](#)

Molecular Identification and Functional Roles of a Ca²⁺–activated K⁺ Channel in Human and Mouse Hearts

J Biol Chem. 2003;278:49085–49094,

[Abstract](#) | [Full Text](#) | [PDF](#)

Comparison of time– and voltage–dependent K⁺ currents in myocytes from left and right atria of adult mice

Am. J. Physiol. Heart Circ. Physiol.. 2003;285:H1837–H1848,

[Abstract](#) | [Full Text](#) | [PDF](#)

Atrial effects of the novel K⁺–channel–blocker AVE0118 in anesthetized pigs

Cardiovasc Res. 2003;60:298–306,

[Abstract](#) | [Full Text](#) | [PDF](#)

Kv1.5 Is an Important Component of Repolarizing K⁺ Current in Canine Atrial Myocytes

Circ. Res.. 2003;93:744–751,

[Abstract](#) | [Full Text](#) | [PDF](#)

Chronic atrial fibrillation does not further decrease outward currents. It increases them.

Am. J. Physiol. Heart Circ. Physiol.. 2003;285:H1378-H1384,
[Abstract](#) | [Full Text](#) | [PDF](#)

Characterisation of the Na, K pump current in atrial cells from patients with and without chronic atrial fibrillation

Cardiovasc Res. 2003;59:593-602,
[Abstract](#) | [Full Text](#) | [PDF](#)

Calcium and potassium currents in cells from adult and aged canine right atria

Cardiovasc Res. 2003;58:526-534,
[Abstract](#) | [Full Text](#) | [PDF](#)

Pharmacological electrical remodelling in human atria induced by chronic β -blockade

Cardiovasc Res. 2003;58:498-500,
[Full Text](#) | [PDF](#)

NO Hope for Patients With Atrial Fibrillation

Circulation. 2002;106:2764-2766,
[Full Text](#) | [PDF](#)

Electrical, contractile and structural remodeling during atrial fibrillation

Cardiovasc Res. 2002;54:230-246,
[Abstract](#) | [Full Text](#) | [PDF](#)

Human inward rectifier potassium channels in chronic and postoperative atrial fibrillation

Cardiovasc Res. 2002;54:397-404,
[Abstract](#) | [Full Text](#) | [PDF](#)

Cellular electrophysiology of atrial fibrillation

Cardiovasc Res. 2002;54:259-269,
[Full Text](#) | [PDF](#)

Analysis of altered gene expression during sustained atrial fibrillation in the goat

Cardiovasc Res. 2002;54:427-437,
[Abstract](#) | [Full Text](#) | [PDF](#)

Cardiac function and electrical remodeling of the calcineurin-overexpressed transgenic mouse

Cardiovasc Res. 2002;54:117-132,
[Abstract](#) | [Full Text](#) | [PDF](#)

Mechanisms of Action of Antiarrhythmic Agent Bertosamil on hKv1.5 Channels and Outward Potassium Current in Human Atrial Myocytes

J. Pharmacol. Exp. Ther.. 2002;300:612-620,

[Abstract](#) | [Full Text](#) | [PDF](#)